Macromolecules

ARTICLE

pubs.acs.org/Macromolecules

Effect of Chain Length on Cytotoxicity and Endocytosis of Cationic Polymers

Jinge Cai,[†] Yanan Yue,[†] Deng Rui,[†] Yanfeng Zhang,[‡] Shiyong Liu,[‡] and Chi Wu*[,†,§]

[†]Department of Chemistry, The Chinese University of Hong Kong, Shatin, N.T., Hong Kong

[‡]CAS Key Laboratory of Soft Matter Chemistry, Department of Polymer Science and Engineering, The University of Science and Technology of China, Hefei, Anhui 230026, China

[§]The Hefei National Laboratory of Physical Science at Microscale, Department of Chemical Physics, The University of Science and Technology of China, Hefei, Anhui 230026, China

ABSTRACT: We investigated the effect of chain length on the cytotoxicity and endocytosis of rhodamine B end-labeled cationic linear poly(2-(*N*,*N*-dimethylamino)ethyl methacrylate) (*RhB*-PDMAEMA) polymers [$M_w = (1.1-4.8) \times 10^4$ g/mol and $M_w/M_n \sim 1.2$], which were synthesized via atom transfer radical polymerization by using rhodamine B-based initiator. The 3-(4,5-dimethylthiazol-2-yl)-2,5-diphenyltetrazolium bromide (MTT), lactate dehydrogenase (LDH), and caspase-3/7 assays revealed that the cytotoxicity and cellular membrane disruption of HepG2 cells induced by PDMAEMA depend on both the polymer concentration and chain length, and the apoptosis depends on chain length at the concentration of 37.6 μg/mL. In the concentration range 10−110 μg/mL, PDMAEMA chains with different lengths are cytotoxic to HepG2 cells by different mechanisms. Namely, (1) for short PDMAEMA chains [$M_w = (1.1-1.7) \times 10^4$ g/mol], the cytotoxicity, membrane disruption, and apoptosis are very low, independent of the chain length; (2) in the medium range ($1.7 \times 10^4 < M_w < 3.9 \times 10^4$ g/mol), the cytotoxicity increases with the chain length and polymer concentration, mainly due to the cooperative effect of membrane disruption and apoptosis; and (3) for long chains [$M_w = (3.9-4.8) \times 10^4$ g/mol], they are very disruptive to the cellular membrane, pro-apoptotic, and able to enter the cytoplasm and nucleus faster than short chains, as revealed by the real-time confocal laser scanning microscopy images, and their much higher cytotoxicity is independent of the PDMAEMA chain length.

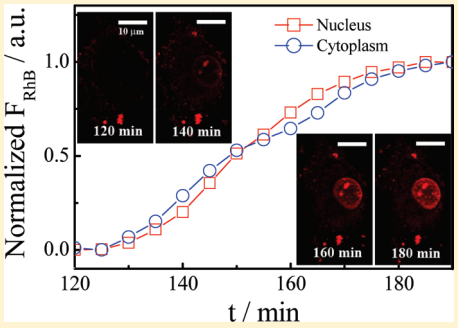

INTRODUCTION

In the gene therapy, exogenous nucleic acids are transferred to targeted cells of patients to express a therapeutic level of defective or deficient proteins.[1−3] The first obstacle in such a gene delivery is the anionic nature of the cellular membrane, preventing the endocytosis of negatively charged DNA.[1] Proper cationic agents (vectors) are needed to (1) condense genetic materials into small particles, (2) protect them against the degradation, and (3) facilitate their cellular entry.[4−6] Cationic polymers are one kind of such nonviral vectors because of their low host immunogenicity, construction flexibility, and facile preparation.[7−11] However, their transfection efficiency is still much lower than that of viral carriers.[12−15] Their cytotoxicity is another important issue that has to be addressed before any applications in human gene therapy.[16−22] Therefore, how to simultaneously increase the transfection efficiency and reduce the cytotoxicity has stood as a very challenging and catch-22 problem in the gene therapy.

To deliver genes from a solution mixture of anionic DNA and cationic polymer all the way through the cellular membrane and cytoplasm into the cell nucleus, the complexes made of polymeric vectors and DNA have to pass through a series of narrow gaps or obstacles (not barriers because one can go over a barrier as long as jumping higher than it), including endocytosis, endolysosomal escape, nuclear transport and entry, and final unpacking of DNA inside the cell nucleus.[1,12,23] The polymer/DNA polyplexes could be blocked by any of these obstacles. Our current study mainly focused on the effect of chain length on the endocytosis and cytotoxicity of cationic polymers. Previous results indicated that the chain length of a given cationic polymer has a significant impact on the cytotoxicity and also on the gene transfection efficiency.[16,24−27] It is generally known that short chains are less cytotoxic than long ones, but the detailed mechanism remains elusive.

Previously, we have experimentally showed that the cytotoxicity increases with the length of a cationic polyethylenimine (PEI) chain even though its structure contains no toxic moieties,[28] which leads us to hypothesize that its cytotoxicity must be physical; namely, cationic charges on the polymer chain interact with negatively charged membranes in both the extracellular and intracellular spaces and complex with negatively charged protein chains in the intracellular space to disrupt their pathways, resulting in the apoptosis.[19,27]

Received: November 3, 2010
Revised: February 16, 2011
Published: March 07, 2011

dx.doi.org/10.1021/ma102498g | *Macromolecules* 2011, 44, 2050–2057

Scheme 1. Synthetic Routes Employed for the Preparation of Rhodamine B End-Labeled Cationic PDMAEMA Polymers with Different Desired Chain Lengths via Atom Transfer Radical Polymerization (ATRP)

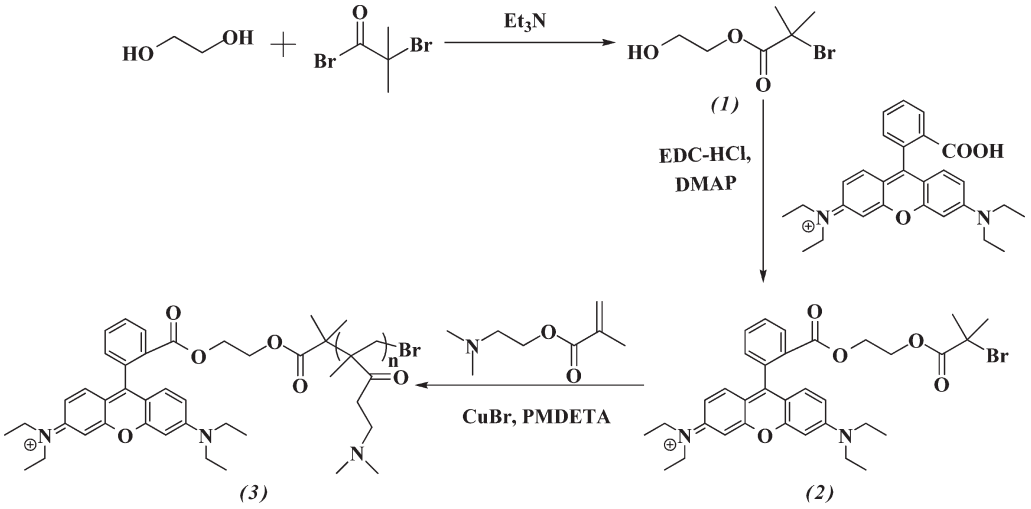

To prove such a hypothesis, we synthesized a series of poly(2-(*N*,*N*-dimethylamino)ethyl methacrylate) (PDMAEMA) chains with different lengths by using atom transfer radical polymerization (ATRP) protocols. Starting from the rhodamine B-based ATRP initiator, PDMAEMA chains were end-labeled with a fluorophore to facilitate real-time cell imaging. Note that PDMAEMA is not a very high efficient gene transfection vector in comparison with other cationic polymers.[18,29] The choice of PDMAEMA is due to its well-documented synthesis and characterization so that it becomes an excellent model for the evaluation of relationships between the chain structures and functions.[4,18,30] Armed with this set of well-characterized polymers, we studied the chain-length-dependent cytotoxicity, cell membrane integrity, and apoptosis, respectively, by using the 3-(4,5-dimethylthiazol-2-yl)-2,5-diphenyltetrazolium bromide (MTT), lactate dehydrogenase (LDH), and caspase-3/7 assays in HepG2 cell line. We also investigated the effect of chain length on the endocytosis kinetics by tracking the HepG2 cellular internalization of the chains with a confocal laser scanning microscope (CLSM).

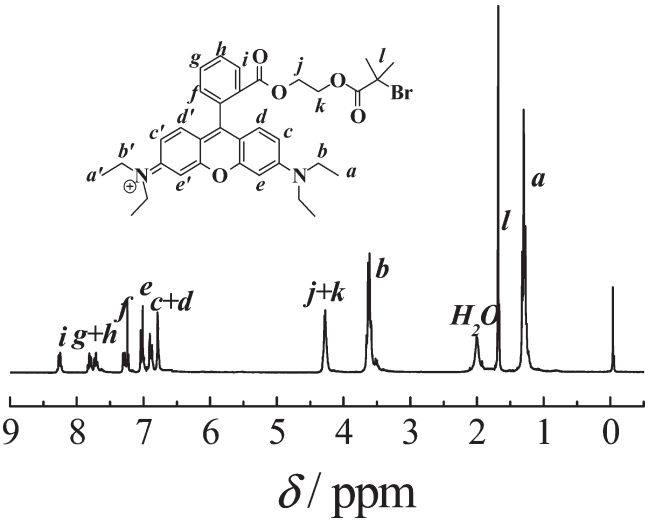

Figure 1. ^{1}H NMR spectrum recorded in $CDCl_3$ for rhodamine B-based ATRP initiator (**2**).

EXPERIMENTAL SECTION

Materials and Cell Lines. 2-(*N*,*N*-Dimethylamino)ethyl methacrylate (DMAEMA, 98%, from Acros, Morris Plains, NJ) was distilled at reduced pressure just prior to use. Rhodamine B (RhB, 99%, from Acros, Morris Plains, NJ) was used without further purification. Cuprous bromide (CuBr, 98%), dimethyl sulfoxide (DMSO), 2-bromo-2-methylpropionyl bromide (98%), and *N*,*N*,*N*′,*N*″,*N*″-pentamethyldiethylenetriamine (PMDETA, 99%) were purchased from Sigma-Aldrich (Deutschland) and used as received. Triethylamine (Et_3N) and ethylene glycol were purchased from the China National Medicines Co. Ltd. and distilled at reduced pressure just prior to use. 1-Ethyl-3-(3-(dimethylamino)propyl)carbodiimide hydrochloride (EDC·HCl, 99%, from GL Biochem Ltd., Shanghai, China) was used as received. Dichloromethane (CH_2Cl_2), 4-(dimethylamino)pyridine (DMAP), isopropanol (IPA), *n*-hexane, methanol, tetrahydrofuran (THF), petroleum ether (30−60 °C), anhydrous sodium sulfate, hydrochloric acid, sodium bicarbonate, and sodium chloride were all purchased from the China National Medicines Co. Ltd. CH_2Cl_2 was dried over CaH_2 and distilled just prior to use and the others were used as received. 3-(4,5-Dimethylthiazol-2-yl)-2,5-diphenyltetrazolium bromide (MTT) and Hoechst 33342 were purchased from Invitrogen (Eugene, OR). CytoTox 96 nonradioactive cytotoxicity assay kit and Caspase-Glo 3/7 assay kit were purchased from Promega (Madison, WI). Fetal bovine serum (FBS), phosphate buffered saline (PBS), Dulbecco's modified Eagle's medium (DMEM), and penicillin−streptomycin were purchased from GIBCO (Grand Island, NY). HepG2 cells were grown at 37 °C, 5% CO_2 in DMEM complete medium, supplemented with 10% FBS, penicillin, and streptomycin (both at 100 units/mL).

PDMAEMA Synthesis. Synthetic routes employed for the preparation of rhodamine B end-labeled cationic PDMAEMA polymers (*RhB*-PDMAEMA) with different desired chain lengths are shown in Scheme 1. First, we prepared 2-hydroxyethyl 2-bromoisobutyrate (**1**) as follows. Into a round-bottom flask equipped with a magnetic stirring bar, ethylene glycol (155.2 g, 2.5 mol) and Et_3N (14.5 mL, 0.1 mol) were charged. After cooling to 0 °C in an ice−water bath, 2-bromoisobutyryl bromide (12.4 mL, 0.1 mol) was added dropwise over ~30 min. The

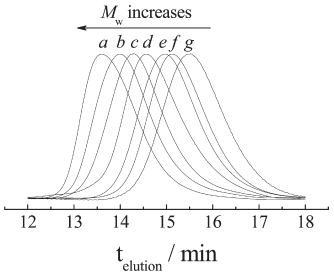

Figure 2. GPC elution profiles recorded for seven rhodamine B-labeled PDMAEMA samples (see Table 1 for average molar masses and polydispersities).

reaction was complete after stirring for another 3 h at room temperature. The mixture was quenched with 1 L of H_2O and extracted with CH_2Cl_2 (100 mL × 3). The combined organic phase was further extracted with deionized water (100 mL × 3). After drying over anhydrous Na_2SO_4, CH_2Cl_2 was removed on a rotary evaporator. The residues were purified by distillation (85 °C, 30 mTorr) to yield a viscous, clear, and colorless liquid (15.6 g, 75%). ^{1}H NMR (300 MHz, $CDCl_3$): δ (TMS, ppm): 4.41 (t, 2H, J = 3.5 Hz), 3.87 (t, 2H, J = 3.3 Hz), 3.21 (s, 1H), 1.95 (s, 6H). ^{13}C NMR (75 MHz, $CDCl_3$): δ (TMS, ppm): 171.80, 67.16, 60.31, 55.72, 30.49.[31]

Then, rhodamine B-based ATRP initiator (**2**) was synthesized by charging rhodamine B (4.8 g, 0.010 mol), EDC·HCl (2.9 g, 0.015 mol), 2-hydroxyethyl 2-bromoisobutyrate (**1**) (3.2 g, 0.015 mol), and dry CH_2Cl_2 (40 mL) into a round-bottom flask equipped with a magnetic stirring bar. After cooling to 0 °C in an ice−water bath, DMAP (1.8 g, 15 μmol) was added. The reaction was conducted at room temperature for 12 h. The reaction mixture was then sequentially extracted with 0.1 M HCl (50 mL × 3), aqueous saturated $NaHCO_3$ (50 mL × 3), and aqueous saturated NaCl solution (50 mL × 3). After drying over anhydrous Na_2SO_4, CH_2Cl_2 was removed on a rotary evaporator. The crude product was purified by column chromatography (first THF/*n*-hexane = 4/1, v/v; then THF/methanol = 10:1, v/v), yielding a purple powder (4.2 g, 65%). ^{1}H NMR ($CDCl_3$, see Figure 1 for peak assignments), δ (TMS, ppm): 8.26 (1H, *i*, aromatic protons), 7.81 (1H, *g*, aromatic protons), 7.71 (1H, *h*, aromatic protons), 7.26 (1H, *f*, aromatic protons), 7.03 (2H, *e*, *e*′, aromatic protons), 6.89 (2H, *c*, *c*′, aromatic protons), 6.79 (2H, *d*, *d*′, aromatic protons), 4.28 (4H, *j*, *k*, $-CH_2CH_2-$), 3.62 (8H, *b*, *b*′, CH_3CH_2-), 1.68 (6H, *l*, $-CH_3$), and 1.30 (12H, *a*, *a*′, CH_3CH_2-).

We finally synthesized a set of narrowly distributed *RhB*-PDMAEMA samples (**3**) by ATRP. In a typical example, DMAEMA (1.258 g, 8.0 mmol), rhodamine B-based initiator (**2**) (0.255 g, 0.4 mmol), PMDETA (69.3 mg, 0.4 mmol), and dry IPA (3.0 mL) were charged into a Schlenk tube. The mixture was degassed by two freeze−pump−thaw cycles. CuBr (57.4 mg, 0.4 mmol) was then introduced into the Schlenk tube under the protection of N_2 flow. The tube was further degassed via three freeze−pump−thaw cycles, sealed under vacuum. After stirring at room temperature for 10 h, the reaction mixture was exposed to air, diluted with THF, and passed through a silica gel column to remove the copper catalysts. After removing the solvents, the residues were dissolved in THF and precipitated into an excess of petroleum ether (30−60 °C). The above dissolution−precipitation cycle was repeated for three times. After drying in a vacuum oven overnight at room temperature, *RhB*-PDMAEMA sample was obtained. GPC analysis gave an M_w of 1.10 × 10^4 and an M_w/M_n of 1.26. Following similar protocols, other *RhB*-PDMAEMA samples with different molar masses were also synthesized by varying the amount of ATRP initiator **2**, and the structural parameters are listed in Table 1.

Sample Characterization. All nuclear magnetic resonance spectroscopy (NMR) spectra were recorded on a Bruker AV300 NMR spectrometer (resonance frequency of 300 MHz for ^{1}H) operated in the Fourier transform mode. $CDCl_3$ was used as the solvents. The gel permeation chromatography (GPC) equipped with a Waters 1515 pump and a Waters 2414 differential refractive index detector (set at 35 °C) was used to determine the molar mass and molar mass distributions. It used a series of three linear Styragel columns HT2, HT4, and HT5 at an oven temperature of 40 °C. The eluent was THF and the flow rate was 1.0 mL/min. A series of narrowly distributed polystyrene (PS) standards were employed for calibration.

3-(4,5-Dimethylthiazol-2-yl)-2,5-diphenyltetrazolium Bromide (MTT) Cell Viability Assay. HepG2 cells were seeded in a 96-well plate at an initial density of 6000 cells/well in 100 μL of the DMEM complete medium. After 24 h, the cells were treated with polymers at varying concentrations. The treated cells were incubated in a humidified environment with 5% CO_2 at 37 °C for 48 h. The MTT reagent (in 20 μL of PBS, 5 mg/mL) was then added to each well. The cells were further incubated for 4 h at 37 °C. The medium in each well was then removed and replaced by 150 μL of DMSO. The plate was gently agitated for 15 min before the absorbance (A) at 490 nm was recorded by a microplate reader (Bio-Rad). The cell viability is calculated as $A_{490,treated}/A_{490,control}$ × 100%, where $A_{490,treated}$ and $A_{490,control}$ are the absorbance values of the cells cultured with and without cationic PDMAEMA, respectively. Each experiment was done in quadruple. The data were shown as the mean value plus a standard deviation (±SD).

It should be noted that when the result from the MTT assay shows low cell viability, there are two possibilities. Namely, the addition of polymer chains inhibits the cellular growth, leading to a low cellular growing rate. In this case, the treated cells will morphologically similar as those in the control group so that the MTT result will not be able to reflect the cytotoxicity. On the other hand, if the low cell viability is due to the cell death, the MTT results do indicate the cytotoxicity because we can see some changes in their morphology. In our study, some of the cells were detached from the plate and began to lyse, revealed by confocal images. Therefore, a combination of the MTT assay and confocal observation should be used.

Table 1. Structural Parameters of Seven Rhodamine B End-Labeled PDMAEMA Samples

RhB-PDMAEMA[a]	DMAEMA monomer (mmol)	initiator **2** (mmol)	M_w (g/mol)[b]	M_w/M_n[b]
sample a	8.0	0.044	4.79×10^4	1.25
sample b	8.0	0.056	3.90×10^4	1.20
sample c	8.0	0.08	3.11×10^4	1.20
sample d	8.0	0.10	2.65×10^4	1.19
sample e	8.0	0.20	1.73×10^4	1.23
sample f	8.0	0.30	1.48×10^4	1.24
sample g	8.0	0.40	1.10×10^4	1.26

[a] All rhodamine B end-labeled PDMAEMA samples were synthesized at a feed ratio of [initiator **2**]:[CuBr]:[PMDETA] = 1:1:1 in IPA (25 °C). [b] Determined by GPC analysis using THF as the eluent.

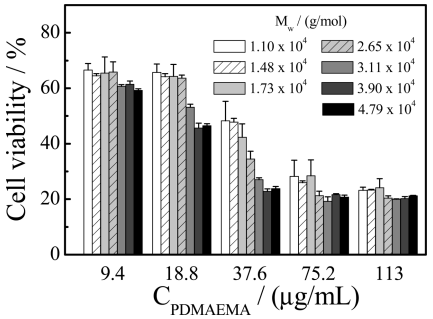

Figure 3. Concentration dependence of HepG2 cell viability of *RhB*-PDMAEMA with different chain lengths, where MTT assay is used.

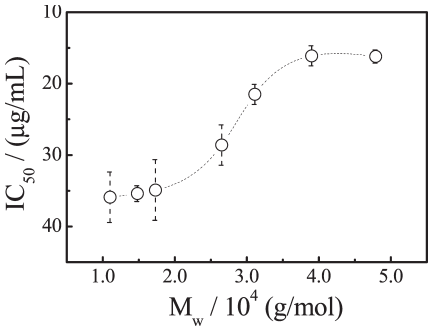

Figure 4. Chain length dependence of half-maximal inhibitory concentration (IC_{50}) of *RhB*-PDMAEMA in HepG2 cells.

It should also be noted that the Trypan blue can also be used to study the cytotoxicity, but it is not able to rapidly process a large number of cells as the MTT assay with a microplate reader. Counting a small number of cells in the trypan blue exclusion may lead to a relatively large error in the results. Therefore, the Trypan blue is not suitable for the study of the cytotoxicity of a large amount of samples. In addition, the λ_{ex} and λ_{em} of PI are 490 and 635 nm, respectively, so that the observation of PI staining will be largely affected by our rhodamine-labeled PDMAEMA that also has a strong absorption at 490 nm and fluoresce in red. This also explains why we used the MTT assay instead of other probes.

Lactate Dehydrogenase (LDH) Membrane Integrity Assay. HepG2 cells were seeded in a 96-well plate at an initial density of 6000 cells/well in 100 μL of the DMEM complete medium. After 24 h, the cells were treated with polymers at different chosen concentrations. The treated cells were incubated in a humidified environment with 5% CO_2 at 37 °C for 4 h. To determine the maximum LDH release, the 10× lysis solution was added to the control group 2 h prior to the use of the CytoTox 96 nonradioactive cytotoxicity assay kit. In each measurement, 50 μL of the cell culture solution from each well of the plate was carefully aspirated and mixed with 50 μL of the reconstituted substrate mix in a new 96-well plate. After 30 min incubation at room temperature, 50 μL of stop solution was added to each well. The absorbance (A) at 490 nm was recorded by a microplate reader (Bio-Rad). The LDH release, defined as $(A_{490,treated} - A_{490,control})/(A_{490,maximum} - A_{490,control}) \times 100\%$, represents the membrane disruption, where $A_{490,treated}$ and $A_{490,control}$ are the absorbance values of the cells cultured in the presence and absence of cationic PDMAEMA, and $A_{490,maximum}$ is the absorbance value of cells in the maximum LDH release control group. Each experiment was conducted in triple. The data were shown as the mean value plus a standard deviation (±SD).

Caspase-3/7 Activity Assay. HepG2 cells were seeded in a 96-well plate at an initial density of 20 000 cells/well in 100 μL of the DMEM complete medium. After 24 h, the cells were treated with polymers at a final concentration of 37.6 μg/mL. The treated cells were incubated in a humidified environment with 5% CO_2 at 37 °C for 4 h. Remove 50 μL of the cell culture medium from each well of 96-well plate. Add 50 μL of the Caspase-Glo 3/7 reagent to each well of the 96-well plate. The plate was gently shaken at room temperature for 2 h before 90 μL of the mix contents of each well was moved to a white-walled 96-well plate. Using a GloMax 96 microplate luminometer, we determined the luminescence from each well. The activity of caspase-3/7 is expressed as $RLU_{treated}/RLU_{control}$, where $RLU_{treated}$ and $RLU_{control}$ are the relative luminescence unit (RLU) of the cells cultured with and without cationic PDMAEMA, respectively. Each experiment was done in quadruple. The data were shown as the mean value plus a standard deviation (±SD).

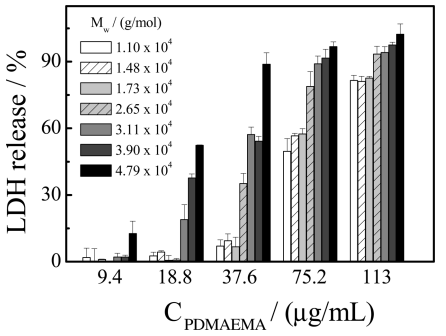

Figure 5. Concentration dependence of LDH release from HepG2 cells treated with *RhB*-PDMAEMA of different chain lengths.

Confocal Laser Scanning Microscopy. A total of 96 000 cells were seeded in a μ-Dish$^{35\ mm,high}$ (ibidi GmbH, Germany). After 24 h, the cellular nucleus was stained with Hoechst for 5 min and then washed once with PBS. After the cell culture medium was aspirated, *RhB*-PDMAEMA in serum-free DMEM was applied at a fixed final concentration (37.6 μg/mL). Live cell imaging was performed for 6 h using a Nikon C1si CLSM equipped with a standard fluorescence detector (Nikon, Japan) and an INU stage-top incubator (Tokai Hit, Japan). Image sequences were captured at an ~5 min interval. *RhB*-PDMAEMA and Hoechst were excited at 543 and 408 nm, respectively. The corresponding emissions were detected at 605/75 and 480/25 nm, respectively. The mean *RhB*-PDMAEMA fluorescence intensities inside the cytoplasm and nucleus are normalized by that in the extracellular space. All the images were analyzed using the Nikon EZ-C1 software.

RESULTS AND DISCUSSION

Figure 3 shows that (1) at $C_{PDMAEMA}$ = 9.4 μg/mL, ~60% of the HepG2 cells are survived, irrespective of the chain length; (2) when $C_{PDMAEMA}$ = 113 μg/mL, only ~20% of the cells are survived, also independent of the chain length; and (3) when 9.4 < $C_{PDMAEMA}$ < 113 μg/mL, the cytotoxicity increases with the chain length. On the other hand, Figure 4 reveals that in the range $M_w < 1.7 \times 10^4$ g/mol, the cytotoxicity of PDMAEMA is low and nearly independent of the chain length, whereas in the range $M_w > 3.9 \times 10^4$ g/mol, the cytotoxicity is rather high but also independent of the chain length. Therefore, for shorter chains ($M_w < 1.7 \times 10^4$ g/mol) and lower concentration ($C_{PDMAEMA}$ < ~10 μg/mL), PDMAEMA is much less cytotoxic; but for longer chains ($M_w > 3.9 \times 10^4$ g/mol) at higher concentrations ($C_{PDMAEMA}$ > ~110 μg/mL), PDMAEMA is fairly cytotoxic, also independent of the chain length. Using the LDH assay, we like to find whether short and long chains are cytotoxic to HepG2 cells in a different way.

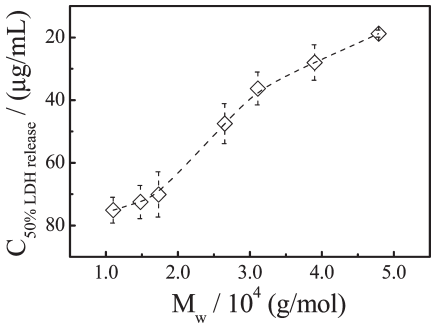

Figure 6. Chain length dependence of *RhB*-PDMAEMA concentration at which LDH release from HepG2 cells reaches 50%.

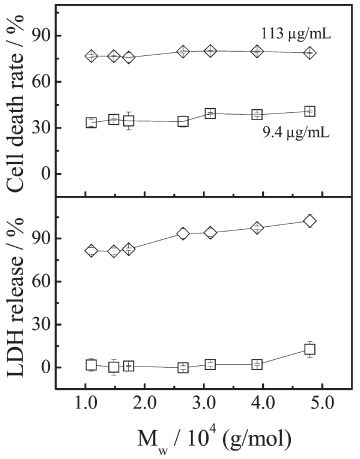

Figure 7. Chain length dependence of HepG2 cell death rate (top) and LDH release (bottom) at low and high *RhB*-PDMAEMA concentrations.

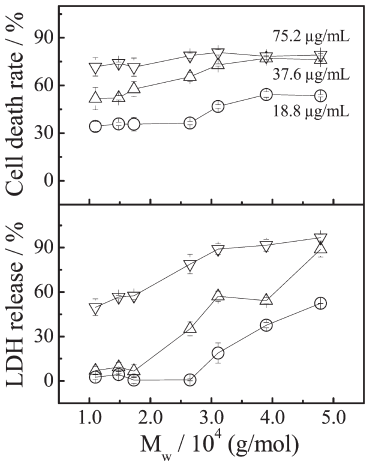

Figure 8. Chain length dependence of HepG2 cell death rate (top) and LDH release (bottom) of *RhB*-PDMAEMA in the middle concentration range.

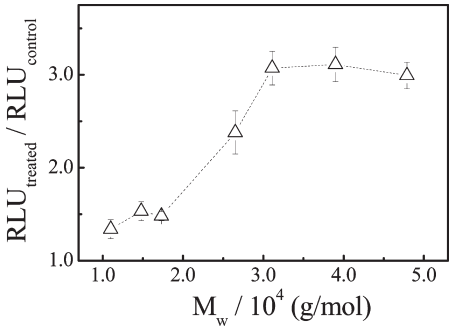

Figure 9. Chain length dependence of caspase-3/7 activity of *RhB*-PDMAEMA at a concentration of 37.6 μg/mL.

Figure 5 shows that when $C_{PDMAEMA}$ = 9.4 μg/mL, PDMAEMA induces a low level release of LDH, independent of the chain length; while in the range 10 < $C_{PDMAEMA}$ < 110 μg/mL, the release level of LDH increases with the chain length, revealing that longer PDMAEMA chains are more disruptive to the cellular membrane than shorter ones. To further illustrate this point, Figure 6 summarizes the chain length dependence of PDMAEMA concentration at which the release of LDH from HepG2 cells reaches 50%, reflecting the ability of different cationic PDMAEMA chains in the destabilization and disruption of the cell membrane. It is clear that the disruption of the cell membrane by shorter chains requires a much higher concentration. In the molar mass range of $(1-5) \times 10^4$ g/mol, the cellular membrane disruption potential of the PDMAEMA chain linearly increases with its length. Figures 3−6 show that both the cytotoxicity and membrane disruption ability of PDMAEMA to HepG2 cells are dependent not only on the chain length but also on the polymer concentration. Therefore, we have to separate theses complicate convolutions in a more clear and understandable way.

Figure 7 shows the chain length dependence of HepG2 cell death rate and the LDH release (membrane disruption) at a low and a high concentration ($C_{PDMAEMA}$ = 9.4 and 113 μg/mL). *RhB*-PDMAEMA is less cytotoxic and nearly not disruptive to the cellular membrane at $C_{PDMAEMA} \leq$ 9.4 μg/mL regardless of its chain length. On the other hand, it becomes highly cytotoxic and its ability to disrupt the cell membrane slightly increases with the chain length when $C_{PDMAEMA} \geq$ 113 μg/mL. In the middle concentration range of 10−110 μg/mL, HepG2 cell death rate and membrane disruption much depend on the chain length, as shown in Figure 8.

For short chains ($M_w < 1.7 \times 10^4$ g/mol), the cytotoxicity and membrane disruption of HepG2 cells are less influenced by their lengths. In the middle range ($1.7 \times 10^4 < M_w < 3.9 \times 10^4$ g/mol), both the cytotoxicity and membrane disruption increase with the chain length. For longer chains ($M_w > 3.9 \times 10^4$ g/mol), the longer the chain, the more disruptive it appears to be, but the cytotoxicity nearly remains a constant. Presumably, longer chains can interact with negatively charged proteins and membranes in the intracellular space more effectively than short ones due to a relatively less entropic loss from the pure thermodynamic point of view.

To find the contribution of apoptosis to cytotoxicity induced by PDMAEMAs with different chain length in the middle concentration range of 10−110 μg/mL, caspase-3/7 activity assay was performed. Caspase-3/7 activity occurs as proteins begin to degrade in the milieu and disappears after cell death.[32]

Figure 9 shows that in the range $M_w < 1.7 \times 10^4$ g/mol the caspase-3/7 activation of treated sample is only 1.5-fold higher than that of untreated control, indicating that apoptosis rate of PDMAEMA is very low. Moreover, no significant difference between these three PDMAEMA chains was observed, revealing

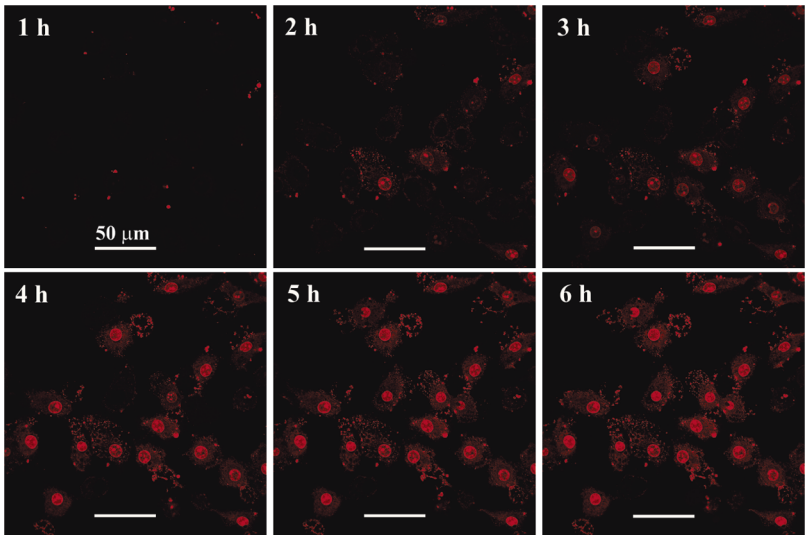

Figure 10. Interpenetration of *RhB*-PDMAEMA chains ($M_w = 1.1 \times 10^4$ g/mol) into HepG2 cells and subsequent intracellular trafficking, where time (t) is counted after addition of *RhB*-PDMAEMA, $C_{PDMAEMA} = 37.6$ μg/mL in serum-free DMEM, and *RhB*-PDMAEMA chains were visualized by excitation with a 543 nm laser light.

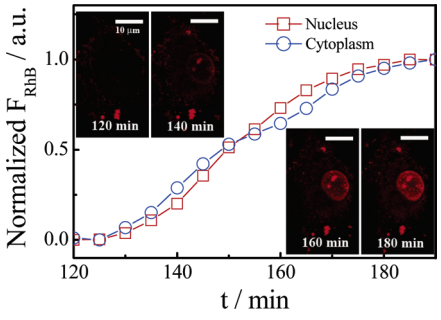

Figure 11. Cellular uptake kinetics of *RhB*-PDMAEMA ($M_w = 1.1 \times 10^4$ g/mol) on one typical HepG2 cell in terms of normalized fluorescence intensity inside nucleus and cytoplasm, respectively, where time (t) is counted after addition of *RhB*-PDMAEMA at a final concentration of 37.6 μg/mL in serum-free DMEM.

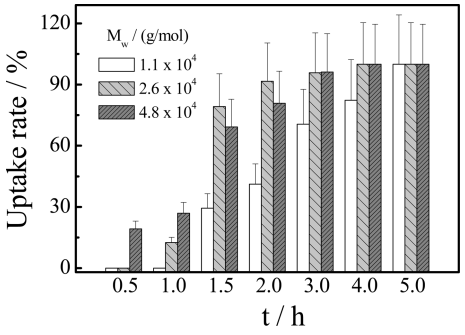

Figure 12. Time dependence of HepG2 cellular uptake of *RhB*-PDMAEMA with different lengths, where 17, 24, and 26 cells are analyzed after adding *RhB*-PDMAEMA with different chain lengths.

that the apoptosis rate is independent of the chain length. In the range 1.7×10^4 g/mol < M_w < 3.9×10^4 g/mol, the apoptosis rate increases with the chain length. In the range $M_w > 3.9 \times 10^4$ g/mol, the apoptosis rate is rather high and almost independent of the chain length.

Therefore, according to Figures 8 and 9, we can conclude that at the concentration of 37.6 μg/mL (1) for short chains (M_w < 1.7×10^4 g/mol), the cytotoxicity, membrane disruption and apoptosis rate of HepG2 cells are less influenced by their lengths; (2) in the middle range 1.7×10^4 g/mol < M_w < 3.9×10^4 g/mol, the cytotoxicity, membrane disruption, and apoptosis rate increase with the chain length, indicating that the cytotoxicity of PDMAEMA in this range might be due to the cooperative effect of apoptosis and the destabilization of the cellular membrane; and (3) for longer chains ($M_w > 3.9 \times 10^4$ g/mol), the longer the chain, the more disruptive it appears to be, whereas the apoptosis rate is not significantly altered, even slightly decreases, so that the cytotoxicity remains a constant, almost independent of the chain length.

Further, we investigated the effect of chain length on HepG2 cellular uptake kinetics. The live cell imaging was recorded for a total of 6 h after the cells were treated with *RhB*-PDMAEMA ($M_w = 1.1 \times 10^4$ g/mol and $C_{PDMAEMA} = 37.6$ μg/mL). Figure 10 shows that as expected the initial uptake times are not identical for different HepG2 cells. However, ~6 h after adding PDMAEMA, both the fluorescence intensities inside the cytoplasm and nucleus reach their maximum values, indicating that the uptake of PDMAEMA ceases after ~6 h for most of the HepG2 cells. To further elucidate the cellular uptake process, we tracked one single cell after the treatment of *RhB*-PDMAEMA ($M_w = 1.1 \times 10^4$ g/mol and $C_{PDMAEMA} = 37.6$ μg/mL). Figure 11 shows that after 120 min *RhB*-PDMAEMA chains form some clumps on the cellular membrane. At 140 min postaddition, the number of the clumps on the membrane increases, and at the same time, both the cytoplasm and the nucleus become faintly fluorescent with some discrete and easily defined patches inside the nucleus. The fluorescence intensity inside the cell, especially for that inside the nucleus, further increases with time. Finally, the overall fluorescence intensity inside the cytoplasm and nucleus approach their maxima after 180 min. Figure 11 also shows the time-dependent fluorescence intensity within the cytoplasm and cell nucleus, revealing the cellular uptake kinetics. The simultaneous increases of the fluorescence intensities inside the cytoplasm and nucleus

dx.doi.org/10.1021/ma102498g |*Macromolecules* 2011, 44, 2050–2057

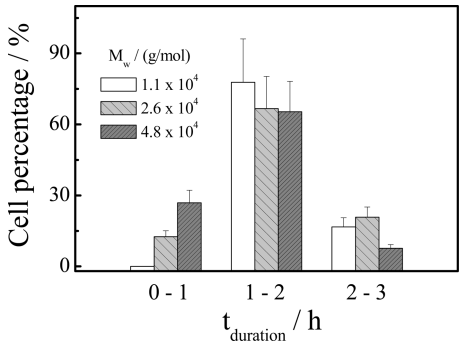

Figure 13. Effect of chain length on HepG2 cellular uptake of *RhB*-PDMAEMA, where *t* is the duration period after adding *RhB*-PDMAEMA, and 17, 24, and 26 cells are analyzed for different chain lengths.

indicate that short *RhB*-PDMAEMA chains can go all the way through the cytoplasm and the nucleus membranes to the nucleus. Moreover, Figure 11 reveals that HepG2 cellular uptake of short *RhB*-PDMAEMA chains only starts at ~120 min after the addition in serum-free DMEM and ends at ~190 min; namely, the whole uptake process occurs within ~3 h. Using such a procedure, we tracked the cellular uptake of 17 cells to obtain distributions and statistics.

Further, we repeated the same kinetic study for longer PDMAEMA chains (M_w = 2.6 × 10^4 and 4.8 × 10^4 g/mol, $C_{PDMAEMA}$ = 37.6 μg/mL) to investigate the effect of chain length on HepG2 cellular uptake. According to the time at which the cellular uptake starts, we analyzed the time-dependent cellular uptake, as shown in Figure 12. For the longest chains, nearly 20% HepG2 cells start to uptake PDMAEMA chains within 0.5 h; for the chains in the middle length range, the cellular uptake starts after 0.5 h and reaches 12% during the first hour; while for the shortest chains, the cellular uptake occurs only after 1 h. Therefore, long chains are more effective in penetrating HepG2 cellular and nuclear membranes. According to how long the cellular uptake lasts, cells are separated into three groups, as shown in Figure 13.

For the longest chains studied, nearly 30% of the cells take 0.5−1.0 h to finish their cellular uptake process; while for the shortest chains, the cellular uptake lasts for more than 1 h. Although the duration time of HepG2 cellular uptake of PDMAEMA chains falls into a wide range of 40−180 min, varying from one cell to another, we can still see that the uptake of longer chains is much faster than that of their short counterparts. This is consistent with the effect of chain length on the cellular membrane disruption. Nevertheless, it is worth noting that HepG2 cellular uptake of either the DNA/PDMAEMA polyplexes or free PDMAEMA chains is much faster than the gene transfection (>12 h); i.e., most of the gene expression occurs afterward.

Finally, we like to emphasize that the purpose of the current study is focused on the effect of polymer chain length on the cytotoxicity not on all the intracellular biochemical markers and other proapoptotic proteins. The detailed pathways of polymer chains with different lengths in the intracellular space have been planned for our future study.

CONCLUSIONS

Using the 3-(4,5-dimethylthiazol-2-yl)-2,5-diphenyltetrazolium bromide (MTT), lactate dehydrogenase (LDH), and caspase-3/7 assays, we have studied the effect of chain length on the cytotoxicity, cellular membrane disruption, and apoptosis of HepG2 cells by using a set of narrowly distributed linear cationic rhodamine B end-labeled poly(2-(*N*,*N*-dimethylamino)ethyl methacrylate) (*RhB*-PDMAEMA) chains with different molar masses [M_w = (1.1−4.8) × 10^4 g/mol]. This systematic study shows that at $C_{PDMAEMA}$ < ~10 μg/mL and $C_{PDMAEMA}$ > ~110 μg/mL, regardless of the chain length, PDMAEMA is less and highly cytotoxic to HepG2 cells, respectively; while in the medium concentration range of 10−110 μg/mL, the cytotoxicity of PDMAEMA to HepG2 cells increases with the chain length but through different mechanisms. Namely, for short chains (M_w < 1.7 × 10^4 g/mol), the cytotoxicity, the membrane disruption ability and apoptosis rate are very low and independent of the chain length; in the medium range of M_w = (1.7−3.9) × 10^4 g/mol, the cytotoxicity is due to the cooperative effect of apoptosis and the destabilization of the cellular membrane; whereas for long chains (M_w > 3.9 × 10^4 g/mol), the membrane disruption and apoptosis rate are rather high, and the pronounced cytotoxicity is also independent of the chain length. Presumably, long cationic chains are more toxic in the intracellular space due to their more effective complexation with negatively charged proteins. The study of the uptake kinetics also shows that long chains can penetrate HepG2 cellular and nuclear membranes more quickly than their short counterparts.

AUTHOR INFORMATION

Corresponding Author

*The Hong Kong address should be used for all correspondence.

ACKNOWLEDGMENT

The financial support of the National Natural Scientific Foundation of China (NNSFC) Projects (50773077 and 20934005) and the Hong Kong Special Administration Region Earmarked (RGC) Projects (CUHK4037/07P, 2160331; CUHK4046/08P, 2160365; CUHK4039/08P, 2160361; and CUHK4042/09P, 2160396) is gratefully acknowledged.

REFERENCES

(1) Pack, D. W.; Hoffman, A. S.; Pun, S.; Stayton, P. S. *Nat. Rev. Drug Discovery* **2005**, *4*, 581–593.
(2) Emery, D. W. *Clin. Appl. Immunol. Rev.* **2004**, *4*, 411–422.
(3) Verma, I. M.; Somia, N. *Nature* **1997**, *389*, 239–242.
(4) Georgiou, T. K.; Vamvakaki, M.; Patrickios, C. S.; Yamasaki, E. N.; Phylactou, L. A. *Biomacromolecules* **2004**, *5*, 2221–2229.
(5) De Smedt, S. C.; Demeester, J.; Hennink, W. E. *Pharm. Res.* **2000**, *17*, 113–126.
(6) Bloomfield, V. A. *Biopolymers* **1997**, *44*, 269–282.
(7) Han, S.; Mahato, R. I.; Sung, Y. K.; Kim, S. W. *Mol. Ther.* **2000**, *2*, 302–317.
(8) Kabanov, A. V. *Pharm. Sci. Technol. Today* **1999**, *2*, 365–372.
(9) Yue, Y.; Jin, F.; Deng, R.; Cai, J.; Chen, Y.; Lin, M.; Kung, H.; Wu, C. *J. Controlled Release* **2011**10.1016/j.jconrel.2010.10.028.
(10) Itaka, K.; Yamauchi, K.; Harada, A.; Nakamura, K.; Kawaguchi, H.; Kataoka, K. *Biomaterials* **2003**, *24*, 4495–4506.
(11) von Harpe, A.; Petersen, H.; Li, Y. X.; Kissel, T. *J. Controlled Release* **2000**, *69*, 309–322.
(12) Morille, M.; Passirani, C.; Vonarbourg, A.; Clavreul, A.; Benoit, J. P. *Biomaterials* **2008**, *29*, 3477–3496.
(13) Schaffert, D.; Wagner, E. *Gene Ther.* **2008**, *15*, 1131–1138.
(14) Read, M. L.; Logan, A.; Seymour, L. W. *Adv Genet.* **2005**, *53*, 19–46.

(15) Wightman, L.; Kircheis, R.; Rossler, V.; Carotta, S.; Ruzicka, R.; Kursa, M.; Wagner, E. *J. Gene Med.* **2001**, *3*, 362–372.
(16) vandeWetering, P.; Cherng, J. Y.; Talsma, H.; Hennink, W. E. *J. Controlled Release* **1997**, *49*, 59–69.
(17) Morimoto, K.; Nishikawa, M.; Kawakami, S.; Nakano, T.; Hattori, Y.; Fumoto, S.; Yamashita, F.; Hashida, M. *Mol. Ther.* **2003**, *7*, 254–261.
(18) Layman, J. M.; Ramirez, S. M.; Green, M. D.; Long, T. E. *Biomacromolecules* **2009**, *10*, 1244–1252.
(19) Parhamifar, L.; Larsen, A. K.; Hunter, A. C.; Andresen, T. L.; Moghimi, S. M. *Soft Matter* **2010**, *6*, 4001–4009.
(20) Fischer, D.; Bieber, T.; Li, Y. X.; Elsasser, H. P.; Kissel, T. *Pharm. Res.* **1999**, *16*, 1273–1279.
(21) Lv, H. T.; Zhang, S. B.; Wang, B.; Cui, S. H.; Yan, J. *J. Controlled Release* **2006**, *114*, 100–109.
(22) Breunig, M.; Lungwitz, U.; Liebl, R.; Goepferich, A. *Proc. Natl. Acad. Sci. U.S.A.* **2007**, *104*, 14454–14459.
(23) Jackson, D. A.; Juranek, S.; Lipps, H. J. *Mol. Ther.* **2006**, *14*, 613–626.
(24) Godbey, W. T.; Wu, K. K.; Mikos, A. G. *J. Biomed. Mater. Res.* **1999**, *45*, 268–275.
(25) Breunig, M.; Lungwitz, U.; Liebl, R.; Fontanari, C.; Klar, J.; Kurtz, A.; Blunk, T.; Goepferich, A. *J. Gene. Med.* **2005**, *7*, 1287–1298.
(26) Georgiou, T. K.; Phylactou, L. A.; Patrickios, C. S. *Biomacromolecules* **2006**, *7*, 3505–3512.
(27) Moghimi, S. M.; Symonds, P.; Murray, J. C.; Hunter, A. C.; Debska, G.; Szewczyk, A. *Mol. Ther.* **2005**, *11*, 990–995.
(28) Deng, R.; Yue, Y.; Jin, F.; Chen, Y. C.; Kung, H. F.; Lin, M. C. M.; Wu, C. *J. Controlled Release* **2009**, *140*, 40–46.
(29) Boussif, O.; Lezoualch, F.; Zanta, M. A.; Mergny, M. D.; Scherman, D.; Demeneix, B.; Behr, J. P. *Proc. Natl Acad. Sci. U.S.A.* **1995**, *92*, 7297–7301.
(30) Cherng, J. Y.; vandeWetering, P.; Talsma, H.; Crommelin, D. J. A.; Hennink, W. E. *Pharm. Res.* **1996**, *13*, 1038–1042.
(31) White, M. A.; Johnson, J. A.; Koberstein, J. T.; Turro, N. J. *J. Am. Chem. Soc.* **2006**, *128*, 11356–11357.
(32) Huang, R.; Southall, N.; Cho, M. H.; Xia, M.; Inglese, J.; Austin, C. P. *Chem. Res. Toxicol.* **2008**, *21*, 659–667.